Article

Probing Stepwise Complexation in Phenylazomethine Dendrimers by a Metallo-Porphyrin Core

Takane Imaoka, Reiko Tanaka, Sachiko Arimoto, Makoto Sakai, Masaaki Fujii, and Kimihisa Yamamoto

J. Am. Chem. Soc., **2005**, 127 (40), 13896-13905• DOI: 10.1021/ja0524797 • Publication Date (Web): 14 September 2005

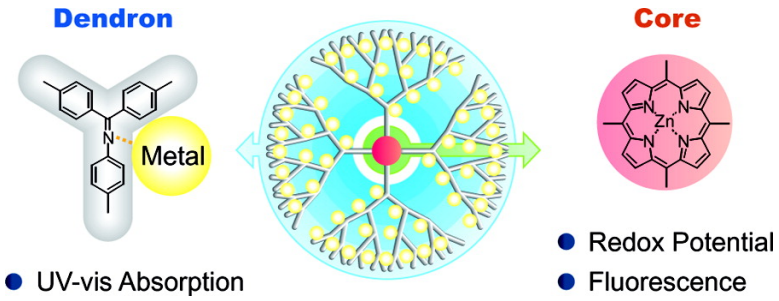

More About This Article

Additional resources and features associated with this article are available within the HTML version:

- Supporting Information
- Links to the 7 articles that cite this article, as of the time of this article download
- Access to high resolution figures
- Links to articles and content related to this article
- Copyright permission to reproduce figures and/or text from this article

View the Full Text HTML

J|A|C|S
ARTICLES
Published on Web 09/14/2005

Probing Stepwise Complexation in Phenylazomethine Dendrimers by a Metallo-Porphyrin Core

Takane Imaoka,† Reiko Tanaka,† Sachiko Arimoto,† Makoto Sakai,‡ Masaaki Fujii,‡ and Kimihisa Yamamoto*,†

Contribution from the Department of Chemistry, Faculty of Science and Technology, Keio University, Yokohama 223-8522, Japan, and Chemical Resources Laboratory, Tokyo Institute of Technology, Yokohama 226-8503, Japan

Received April 16, 2005; E-mail: yamamoto@chem.keio.ac.jp

Abstract: A series of dendritic phenylazomethines (DPA), which have a *meso*-substituted zinc porphyrin core (**DPAGX-ZnP**, X = 1−4), were synthesized. Structural studies of these dendrimers were carried out using Tri-SEC (triple detection after size exclusion chromatography), intrinsic viscosity analysis, TEM (tunneling electron microscopy), and molecular modeling calculations by AM1. As a result, a sphere-like structure within a single-nanometer scale (R_h = 22 Å for **DPAG4-ZnP**) was observed. In addition, encapsulating effects by the DPA shell in the larger dendrimers were confirmed as fundamental properties, based on the UV−vis abosorption spectra, cyclic voltammograms, and ^{1}H NMR spin−lattice relaxation times (T_1). The **DPAGX-ZnP** acts as a multi-metal ion reservoir for $SnCl_2$ and $FeCl_3$. The generation-4 dendrimer (**DPAG4-ZnP**) can take up to 60 molar amounts of metal complexes around the porphyrin core. A quantitative study of the metal assembling reaction by UV−vis titration revealed stepwise layer-by-layer complexations from the inner imines nearest to the core to the surface. The redox behavior and fluorescence of the zinc porphyrin in these metal-assembled dendrimers also support the stepwise complexation of the metal ion. These analyses suggest that the finely assembled metal complexes in a dendrimer architecture strongly affect the electronic status of the porphyrin core. Results from transient absorption measurements strongly indicate a very fast electron transfer on a subpicosecond time scale between the core and assembled metal complexes.

Introduction

Dendritic macromolecules[1] having appropriate ligands as their backbone structure can assemble multiple metal complexes in themselves through complexation. They are a new class of macromolecular complexes, which has less dispersion in their molecular structure than the conventional macromolecular−metal complexes.[2] Metallo-dendrimers[3] have been extensively studied in recent years, because of their structural variety and potential for applications. Many kinds of metal complexes with a dendritic architecture are actually reported and utilized as catalysts,[4,5] sensors,[6] and a molecular flask[7] for metal cluster synthesis. For their applications, the number and the position of the metal complexes are essential factors controlling these functions.

† Keio University.
‡ Tokyo Institute of Technology.

(1) A synthetic macromolecules with no structural dispersion. For selected reviews, see: (a) Tomalia, D. A.; Naylor, A. M.; Goddard, W. A., III. *Angew. Chem., Int. Ed. Engl.* **1990**, *29*, 138−175. (b) Zeng, F.; Zimmerman, S. C. *Chem. Rev.* **1997**, *97*, 1681−1712. (c) Fischer, M.; Vögtle, F. *Angew. Chem., Int. Ed.* **1999**, *38*, 885−905. (d) Majoral, J.-P.; Caminade, A.-M. *Chem. Rev.* **1999**, *99*, 845−880. (e) Bosman, A. W.; Janssen, H. M.; Meijer, E. W. *Chem. Rev.* **1999**, *99*, 1665−1688. (f) Vögtle, F.; Gestermann, S.; Hesse, R.; Schwierz, H.; Windisch, B. *Prog. Polym. Sci.* **2000**, *25*, 987−1041. (g) Hecht, S.; Fréchet, J. M. J. *Angew. Chem., Int. Ed.* **2001**, *40*, 74−91. (h) Fréchet, J. M. J.; Tomalia, D. A. *Dendrimers and other Dendritic Polymers*; John Wiley & Sons: New York, 2002. (i) Newkome, G. R.; Moorefield, C. N.; Vögtle, F. *Dendrimers and Dendrons: Concepts, Synthesis, Applications*; Wiley−VCH: Weinheim, 2001.

(2) *Macromolecule-metal Complexes*; Ciardelli, F., Tsuchida, E., Wohrle, D., Eds.; Springer: New York, 1996.

(3) Many dendrimers containing metal complexes are reported. They can be seen in the following review: Newkome, G. R.; He, E.; Moorefield, C. N. *Chem. Rev.* **1999**, *99*, 1689−1746.

(4) (a) Bhyrappa, P.; Young, J. K.; Moore, J. S.; Suslick, K. S. *J. Am. Chem. Soc.* **1996**, *118*, 5708−5711. (b) Kimura, M.; Shiba, T.; Yamazaki, M.; Hanabusa, K.; Shirai, H.; Kobayashi, N. *J. Am. Chem. Soc.* **1999**, *121*, 5636−5642. (c) Uyemura, M.; Aida, T. *J. Am. Chem. Soc.* **2002**, *124*, 11392−11403. (d) Uyemura, M.; Aida, T. *Chem.-Eur. J.* **2003**, *9*, 3492−3500.

(5) (a) Brunner, H. *J. Organomet. Chem.* **1995**, *500*, 39−46. (b) Chow, H.-F.; Mak, C. C. *J. Org. Chem.* **1997**, *62*, 5116−5127. (c) Rheiner, P. B.; Seebach, D. *Chem.-Eur. J.* **1999**, *5*, 3221−3236. (d) Kimura, M.; Sugihara, Y.; Muto, T.; Hanabusa, K.; Shirai, H.; Kobayashi, N. *Chem.-Eur. J.* **1999**, *5*, 3495−3500. (e) Sen, A.; Suslick, K. S. *J. Am. Chem. Soc.* **2000**, *122*, 11565−11566. (f) Hecht, S.; Fréchet, J. M. J. *J. Am. Chem. Soc.* **2001**, *123*, 6959−6960. (g) Astruc, D.; Chardac, F. *Chem. Rev.* **2001**, *101*, 2991−3023. (h) Twyman, L. J.; King. A. S. H.; Martin, I. K. *Chem. Soc. Rev.* **2002**, *31*, 69−82.

(6) (a) Valério, C.; Alonso, E.; Ruiz, J.; Blais, J.-C.; Astruc, D. *Angew. Chem., Int. Ed.* **1999**, *38*, 1747−1751. (b) Daniel, M.-C.; Ruiz, J.; Blais, J.-C.; Daro, N.; Astruc, D. *Chem.-Eur. J.* **2003**, *9*, 4371−4379. (c) Valério, C.; Fillaut, J.-L.; Ruiz, J.; Guittard, J.; Blais, J.-C.; Astruc, D. *J. Am. Chem. Soc.* **1997**, *119*, 2588−2589. (d) Daniel, M.-C.; Ruiz, J.; Nlate, S.; Blais, J.-C.; Astruc, D. *J. Am. Chem. Soc.* **2003**, *125*, 2617−2628.

(7) (a) Crooks, R. M.; Zhao, M.; Sun, L.; Chechik, V.; Yeung, L. K. *Acc. Chem. Res.* **2001**, *34*, 181−190. (b) Zhao, M.; Crooks, R. M. *Adv. Mater.* **1999**, *11*, 217−220. (c) Zhao, M.; Crooks, R. M. *Angew. Chem., Int. Ed.* **1999**, *38*, 364−366. (d) Zhao, M.; Sun, L.; Crooks, R. M. *J. Am. Chem. Soc.* **1998**, *120*, 4877−4878. (e) Chechik, V.; Crooks, R. M. *J. Am. Chem. Soc.* **2000**, *122*, 1243−1244. (f) Lang, H.; May, R. A.; Iversen, B. L.; Chandler, B. D. *J. Am. Chem. Soc.* **2003**, *125*, 14832−14836. (g) Ooe, M.; Murata, M.; Mizugaki, T.; Ebitani, K.; Kaneda, K. *J. Am. Chem. Soc.* **2004**, *126*, 1604−1605. (h) Balogh, L.; Tomalia, D. A. *J. Am. Chem. Soc.* **1998**, *120*, 7355−7356.

10.1021/ja0524797 CCC: $30.25

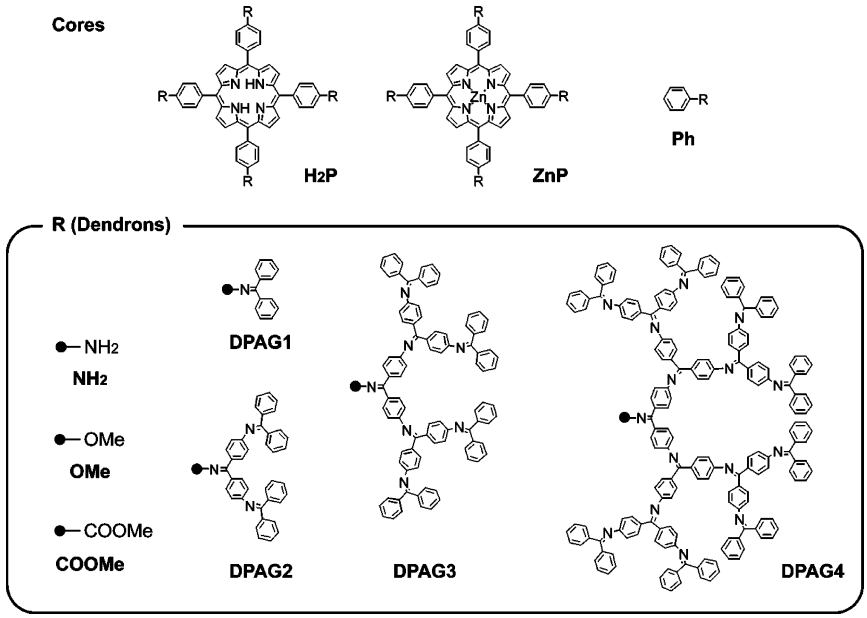

Figure 1. Chemical structures of DPA-substituted poprhyrins and related model compounds.

Dendritic phenylazomethines (DPA) are also one of the Shiff-base ligands bearing multiple imine (C═N) units as coordination sites. They are unusual macromolecules in which multiple metal ions are finely assembled as if they recognize the layers to coordinate.[8] This unique property is a characteristic of the DPA. It enables the dendrimer to assemble metal complexes with complete control of the number and position of the metal ion at any metal/dendrimer equivalents ratio, while other dendrimers cannot define them until full complexation.[9] We have previously reported novel DPAs having a cobalt porphyrin core that act as a catalyst for CO_2 reduction with a very low overpotential.[10] It is based on the synergetic effect of the precisely assembled metal complexes with a porphyrin core involving multi-electron-transfer processes.

The aim of this work is to establish the methodology for the precise assembly around the functional core unit such as porphyrin complexes. In this paper, we report the synthesis of phenylazomethine dendrimers having a metallo-porphyrin core (Figure 1) and the stepwise assembly of metal ions. The porphyrins are not only available as a center of chemical functions (e.g., catalysts or photosensitizer), but also as a molecular probe of the external environment such as solvents or ionic strengths. We employed the UV−vis absorption, redox potential, and fluorescence intensity as probes for characterization of the metal assembly and their effect on the electronic status of the core.

Results and Discussion

Synthesis of Dendritic Phenylazomethines with a Porphyrin Core. The phenylazomethine dendrimers with a free-base porphyrin core (**DPAGX-H_2P**, X = 1−4) were synthesized from *meso*-tetrakis(*p*-aminophenyl)porphine[11] and the corresponding phenylazomethine dendrons[12] (generation number = 1−4) using $TiCl_4$ as the dehydrating reagent by the convergent approach.[13] The reaction was almost completed within 3 h with an excess amount of dendrons and $TiCl_4$, but a side product appeared after a longer reaction time. The side product was found to be a titanyl (Ti═O) porphyrin derivative and half-finished (di- or trisubstituted) products based on the MALDI-TOF-mass and fluorescence spectra.[14] After purification of these products using silica gel chromatography and preparative HPLC with a GPC column, all of the free-base porphyrin dendrimers (**DPAGX-H_2P**) were characterized by ^{1}H, ^{13}C NMR, MALDI-TOF-mass spectrometries and elemental analysis. The zinc-porphyrin dendrimers (**DPAGX-ZnP**, X = 1−4) were synthesized by zinc insertion into the **DPAGX-H_2P** using excess amounts of $Zn(OAc)_2$ in THF in the presence of triethylamine (Et_3N). The reaction completeness was confirmed by monitoring the absorption spectral changes of the Q-bands (550−650 nm). The $Zn(OAc)_2$ did not coordinate to the phenylazomethine dendron, because excess amounts of Et_3N were added to the solution, which prevents complexation with the dendron units. This is confirmed by no UV−vis absorption change around 300−400 nm, which is attributed to the $\pi-\pi^*$ bands of the phenylazomethine dendron.

Structural Analysis. We attempted to determine the structural characteristics of **DPAGX-H_2P**. To obtain a complete

(8) (a) Yamamoto, K.; Higuchi, M.; Shiki, S.; Tsuruta, M.; Chiba, H. *Nature* **2002**, *415*, 509−511. (b) Imaoka, T.; Horiguthi, H.; Yamamoto, K. *J. Am. Chem. Soc.* **2003**, *125*, 340−341. (c) Enoki, O.; Imaoka, T.; Yamamoto, K. *Org. Lett.* **2003**, *5*, 2547−2549. (d) Satoh, N.; Cho, J.-S.; Higuchi, M.; Yamamoto, K. *J. Am. Chem. Soc.* **2003**, *125*, 8104−8105. (e) Higuchi, M.; Tsuruta, M.; Chiba, H.; Shiki, S.; Yamamoto, K. *J. Am. Chem. Soc.* **2003**, *125*, 9988−9997. (f) Yamamoto, K.; Higuchi, M.; Kimoto, A.; Imaoka, T.; Masachika, K. *Bull. Chem. Soc. Jpn.* **2005**, *78*, 349−355.

(9) (a) Tominaga, M.; Hosogi, J.; Konishi, K.; Aida, T. *Chem. Commun.* **2000**, 719−720. (b) Klein Gebbink, R. J. M.; Bosman, A. W.; Feiters, M. C.; Meijer, E. W.; Nolte, R. J. M. *Chem.-Eur. J.* **1999**, *5*, 65−69. (c) Ottaviani, M. F.; Montalti, F.; Turro, N. J.; Tomalia, D. A. *J. Phys. Chem. B* **1997**, *101*, 158−166. (d) Ottaviani, M. F.; Bossmann, S.; Turro, N. J.; Tomalia, D. A. *J. Am. Chem. Soc.* **1994**, *116*, 661−671. (e) Vögtle, F.; Gestermann, S.; Kauffmann, C.; Ceroni, P.; Vicinelli, V.; Balzani, V. *J. Am. Chem. Soc.* **2000**, *122*, 10398−10404. (f) Vicinelli, V.; Ceroni, P.; Maestri, M.; Balzani, V.; Gorka, M.; Vögtle, F. *J. Am. Chem. Soc.* **2002**, *124*, 6461−6468. (g) Cohen, S. M.; Petoud, S.; Raymond, K. N. *Chem.-Eur. J.* **2001**, *7*, 272−279. (h) Grabchev, I.; Chovelon, J.-M.; Qian, X. *New J. Chem.* **2003**, *27*, 337−340.

(10) The description is mainly noted in the Supporting Information of ref 8b.

(11) Bettelheim, A.; White, B. A.; Raybuck, S. A.; Murray, R. W. *Inorg. Chem.* **1987**, *26*, 1009−1017.

(12) Takanashi, K.; Chiba, H.; Higuchi, M.; Yamamoto, K. *Org. Lett.* **2004**, *6*, 1709−1712.

(13) Fréchet, J. M. J. *Science* **1994**, *263*, 1710−1715.

(14) The fluorescence of the titanyl porphyrin appeared around 600 nm upon an excitation at 540 nm (porphyrin Q-band), while the free-base porphyrin showed a fluorescence around 650 nm.

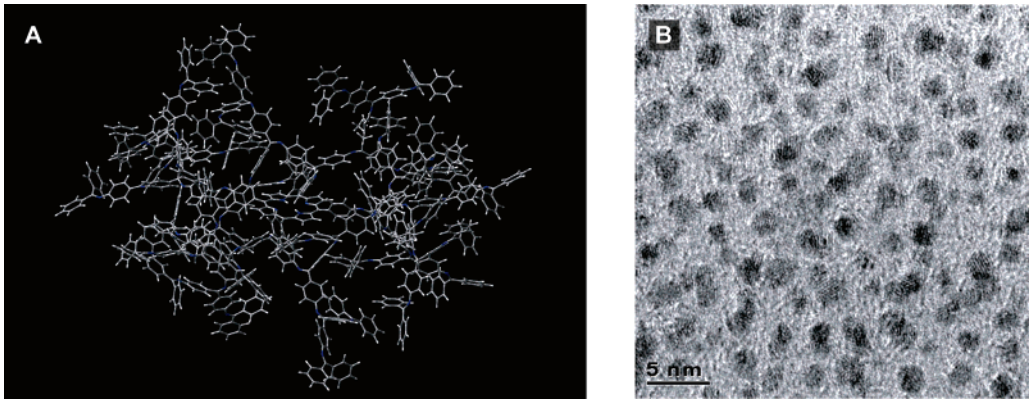

Figure 2. (A) A 3D model of **DPAG4-H$_2$P** optimized by a MOPAC (AM1) calculation, and (B) a transmission electron microscopy image of **DPAG4-ZnP** stained by RuO_4 vapor.

Table 1. Hydrodynamic Radii and Fundamental Properties of **DPAGX-Zn**

		λ_{max} (nm)[b]		$E_{1/2}$ (V vs Fc/Fc$^+$)[c]				
dendrimer	R_h (Å)[a,f]	$CHCl_3$	THF	$CHCl_3$–MeCN[g]	THF	k_0 (cm^{-1} s^{-1})[d,f]	T_1 (s)[e]	T_2 (s)[e]
DPAG1-ZnP	9.6	429, 554, 596	431, 560, 603	0.34	0.40	2.6×10^{-2}	2.03	0.74
DPAG2-ZnP	13.4	433, 556, 599	434, 561, 604	0.33	0.39	1.8×10^{-2}	2.40	0.61
DPAG3-ZnP	17.5	435, 556, 599	436, 560, 603	0.32	0.37	6.5×10^{-3}	2.77	0.27
DPAG4-ZnP	22.0	437, 559, 602	438, 560, 604	0.26	0.34	5.9×10^{-4}	3.06	0.11

[a] Hydrodynamic radii. [b] UV−vis absorption maximum wavelengths. [c] Half-wave (standard redox) potentials of ZnP/ZnP$^+$ couple. [d] Standard rate constants of heterogeneous redox reactions on GCE. [e] Spin−lattice and spin−spin relaxation times of β protons on the porphyrin ring in $CDCl_3$. [f] In THF. [g] Mixing ratio at 4:1 (v/v).

image of the dendrimer, we employed a semiempirical molecular orbital calculation (AM1) to optimize the conformational structure. The resulting structure showed that the dendrimer has a space, which might allow it to encapsulate small molecules (Figure 2A). The four dendrons spread in three-dimensional directions from the porphyrin core, and the terminal-to-terminal distance between each opposite side is about 5 nm. The porphyrin core seems to be more accessible than that of the benzyl ether dendrimers.[15] This reflects the rigid π-conjugating backbone of the phenylazomethines.

The structural information in the solution phase was experimentally studied using the Tri-SEC (triple detection after the size exclusion chromatography) technique. The elution curve of the **DPAGX-ZnP** detected by the refractive index (RI) showed a symmetric peak corresponding to mono-dispersion in the molecular hydrodynamic radii for each generation number (X). The same retention time of **DPAGX-ZnP** from **DPAGX-H$_2$P** or **DPAGX-CoP** suggests independence of the entire structure by a metal ion chelating into the porphyrin ring.

Triple detection by RI (refractive index), LS (light scattering), and IV (intrinsic viscosity) after the separation by SEC provides information about the molecular weight (M_w), hydrodynamic radius (R_h), and morphology.[16] In general, the M_w can be derived from a combination of the RI and LS measurements, and the morphology of a molecule can be predicted from the slope of the Mark−Houwink Sakurada plot.[17] However, the LS measurement was not available for the dendrimers due to the strong fluorescence from the porphyrin core. Therefore, we employed the M_w values from the MALDI-TOF-MS measurements instead of the LS. The intrinsic viscosity [η] was almost constant for dendrimers G2−G4. This indicates a sphere-like structure for **DPAGX-ZnP** when the generation number is greater than 2. In a previous case, DPA with a triphenylamine (**DPAGX-TPA**) core also became spherical when the generation number was greater than 2.[8d] The plateau value of [η] for the dendrimer with a porphyrin core is smaller than that with the trithiophenylphenylamine (TPA) core. These results suggest that the structural density of **DPAGX-ZnP** is higher than that of **DPAGX-TPA**, because the substitution number (4 for **ZnP**, 3 for **TPA**) is higher despite almost the same size core unit. While the intrinsic viscosity of the benzyl ether dendrimers with a porphyrin core reached the maximum at the second or third generation,[18] the phenylazomethine dendrimers did not show a maximum point up to the fourth generation. This result can be explained by the structural flexibility of the DPA being more rigid than that of the benzyl ether dendrimers.[19]

The hydrodynamic radius (R_h) in solution can be calculated by the following equation using the M_w and [η] (from IV) values.

$$[\eta] = 2.5N_a(4\pi R_h^3/3M_w) \quad (1)$$

The R_h values calculated using eq 1 are listed in Table 1. This could also be estimated from the diffusion coefficient, which is generally obtained by an electrochemical method or PFGSE NMR.[20] Here, we employed cyclic voltammetry by comparing the experiment with digital simulations. Although the fitting

(15) Tomoyose, Y.; Jiang, D.-L.; Jin, R.-H.; Aida, T.; Yamashita, T.; Horie, K.; Yashima, E.; Okamoto, Y. *Macromolecules* **1996**, *29*, 5236−5328.
(16) Bahary, W. S.; Hogan, N. P.; Jilani, M.; Aronson, M. P. In *Advances in Chemistry Series*; *Chromatographic Characterization of Polymers*; Provder, T., Barth, H. G., Urban, M. W., Eds.; American Chemical Society: Washington, DC, 1995; Vol. 247, pp 151−166.
(17) Billmeyer, F. W., Jr. *Textbook of Polymer Science*, 3rd ed.; John Wiley & Sons: New York, 1984; p 208.
(18) Matos, M. S.; Hofkens, J.; Verheijen, W.; De Schryver, F. C.; Hecht, S.; Pollak, K. W.; Fréchet, J. M. J.; Forier, B.; Dehaen, W. *Macromolecules* **2000**, *33*, 2967−2973.
(19) (a) Boris, D.; Rubinstein, M. *Macromolecules* **1996**, *29*, 7251−7260. (b) Cavallo, L.; Fraternali, F. *Chem.-Eur. J.* **1998**, *4*, 927−934. (c) Ballauff, M.; Likos, C. N. *Angew. Chem., Int. Ed.* **2004**, *43*, 2998−3020.

failed for **DPAG4-ZnP** because of a large shell effect, the values from G1 to G3 were consistent with that from the SEC experiment. The linear relationship between the hydrodynamic volume ($V_h = 4\pi R_h^3/3$) and the molecular weight (M_w) is evidence for the fixed density of the backbone structure. The sizes of the **DPAGX-ZnP** were almost equal to those of **DPAGX-TPA** when the generation numbers (X) are the same. They are evidence that the polyphenylazomethine structure is rigid and is not bent in solvents. This idea may also be supported by the fact that their growth in diameter with the generation number increase is linear, whereas such growth for the benzyl ether dendrimer is limited.[18]

The direct observation of the **DPAG4-ZnP** was carried out by TEM (transmission electron microscopy). As can be seen in Figure 2B, the dendrimer stained with RuO_4 showed a round shape shadow with a 2.7 nm diameter, which is certainly larger than that of the phenylazomethine dendrimer with a *p*-phenylene core (**DPAG4-PPh**: 2.3 nm). The size is relatively smaller than the hydrodynamic radius, because it is a stained image, which does not exactly match the actual dendrimer.[21]

Encapsulation of the Porphyrin Core. An encapsulating effect, which is commonly observed in dendrimers,[1g] can be confirmed as a property of the porphyrin core. The UV−vis absorption of these zinc porphyrins (Soret bands), which were red-shifted by the increasing generation number, reflects the π orbital interaction between the core and dendrons (Table 1). The solvent dependence of the porphyrin Q-bands clearly indicates the exclusion of solvent molecules around the core, because the difference in the absorption maximum wavelength for each solvent becomes smaller by increasing the generation number.[22] The redox wave of the ZnP/ZnP^+ couple on the cyclic voltammograms became broad and small with the increasing generation number. A decreasing electron-transfer rate constant (k_0) is a common feature observed in large dendritic molecules having a redox-active core.[23] In these molecules, a redox potential shift is also a characteristic; in particular, the ZnP/ZnP^+ redox couple shifts in the negative direction with the generation number (Table 1).[23a] These phenomena were considered to be based on the dendritic branches creating a microenvironment in which solvent molecules are excluded. The standard rate constants (k_0) of the redox reactions on an electrode surface were estimated by Nicholson's analysis.[23e,24] The obvious attenuation of the rate constant with the change in the generation number (X) is related to the encapsulating effect of the porphyrin core. In addition, the values of the ^{1}H NMR longitudinal (spin−lattice) relaxation time (T_1) of the porphyrin β protons in higher generation number dendrimers are longer (Table 1), suggesting that the steric factor prevents solvent molecules from approaching the core.[4d,15,25] However, the transverse relaxation times (T_2), which involve a spin−spin relaxation mechanism,[26] showed the opposite trend to T_1. The shorter T_2 values of the larger dendrimers may reflect an acceleration of the spin−spin coupling with aromatic protons on the peripheral dendrons.

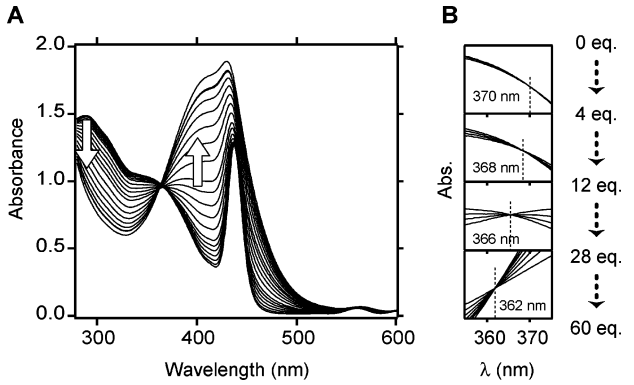

Figure 3. (A) UV−vis absorption spectra changes of **DPAG4-ZnP** (2.5 μM) in C_6H_6/MeCN (1:1) upon the addition of $SnCl_2$, and (B) enlargements of the spectra at the isosbestic points.

Spectroscopic Characterization of Metal Coordination to the Dendritic Backbone. We have previously reported the stepwise complexation from imines nearest to the cobalt porphyrin core in a phenylazomethine dendrimer.[8b] The complexation was accompanied by a color change, which is measured by UV−vis spectra measurements. The addition of $SnCl_2$ to a benzene/acetonitrile solution of **DPAG4-ZnP** also results in a change in the solution color from light yellow to deep orange. The UV−vis absorption spectral changes were similar to that of the complexation of $SnCl_2$ with **DPAGX-PPh**[8a] and **DPAGX-CoP**.[8b] To determine the details of the $SnCl_2$ coordination with the dendrimer, we measured the UV−vis absorption changes upon the addition of a small portion of equimolar $SnCl_2$. The time course of the absorption reached equilibrium within 10 min after the addition of $SnCl_2$; that is, the complexation equilibrium should be accomplished in several minutes for each drop of $SnCl_2$ upon titration. During the addition, the absorption around 320 nm attributed to the free-base phenylazomethines decreased, and that around 400 nm attributed to the metal complexes increased (Figure 3A). Finally, the change reached saturation after the addition of 60 equiv of $SnCl_2$, in which every imine site in the dendrimer was filled.

The isosbestic point accompanying the spectral changes shifted during the addition of the 60 equiv of $SnCl_2$ (Figure 3B). Consequently, four independent isosbestic points appeared in turn. An isosbestic point first appeared at 370 nm up to the addition of four-molar amounts of $SnCl_2$ and then shifted to 368 nm between 5 and 12 equiv. Again, it appeared at 363 nm between 13 and 28 equiv of $SnCl_2$. Finally, it was at 361 nm when more than 32 equiv of $SnCl_2$ was added. This result suggests that four kinds of $SnCl_2$−imine complexes are successively formed from the root imines (nearest to the core) to the terminals (the farthest from the core), because the molar amounts required to move the isosbestic points agreed with the number of imines on each layer (Scheme 1).

(20) (a) Cardona, C. M.; Kaifer, A. E. *J. Am. Chem. Soc*. **1998**, *120*, 4023−4024. (b) Gorman, C. B.; Smith, J. C.; Hager, M. W.; Parkhurst, B. L.; Sierzputowska-Gracz, H.; Haney, C. A. *J. Am. Chem. Soc.* **1999**, *121*, 9958−9966. (c) Goldsmith, J. I.; Takada, K.; Abruña, H. D. *J. Phys. Chem. B* **2002**, *106*, 8504−8513.
(21) Higuchi, M.; Shiki, S.; Ariga, K.; Yamamoto, K. *J. Am. Chem. Soc*. **2001**, *123*, 4414−4420.
(22) Hecht, S.; Vladimirov, N.; Fréchet, J. M. J. *J. Am. Chem. Soc.* **2001**, *123*, 18−25.
(23) (a) Dandliker, P. J.; Diederich, F.; Gross, M.; Knobler, C. B.; Louati, A.; Sanford, E. M. *Angew. Chem., Int. Ed. Engl*. **1994**, *33*, 1739−1742. (b) Pollak, K. W.; Leon, J. W.; Fréchet, J. M. J.; Maskus, M.; Abruña, H. D. *Chem. Mater*. **1998**, *10*, 30−38. (c) Weyermann, P.; Gisselbrecht, J.-P.; Boudon, C.; Diederich, F.; Gross, M. *Angew. Chem., Int. Ed*. **1999**, *38*, 3215−3219. (d) Gorman, C. B.; Smith, J. C. *Acc. Chem. Res*. **2001**, *34*, 60−71. (e) Chasse, T. L.; Sachdeva, R.; Li, Q.; Li, Z.; Petrie, R. J.; Gorman, C. B. *J. Am. Chem. Soc*. **2003**, *125*, 8250−8254.
(24) Nicholson, R. S. *Anal. Chem.* **1965**, *37*, 1351−1355.
(25) Hecht, S.; Fréchet, J. M. J. *J. Am. Chem. Soc.* **1999**, *121*, 4084−4085.
(26) Traficante, D. D. In *Encyclopedia of Nuclear Magnetic Resonance*; Grant, D. M., Harris, R. K., Eds.; John Wiley: New York, 1996; Vol. 6, pp 3988−4003.

Scheme 1. Schematic Representation of the Stepwise Complexation to **DPAG4-ZnP**

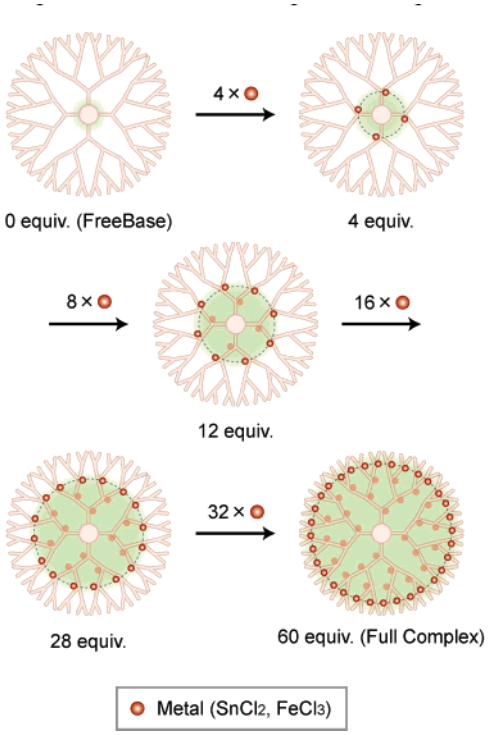

In the dendrimer with a different generation number (X = 1−3), a similar successive coordination takes place. During the stepwise addition of $SnCl_2$ to the **DPAG3-ZnP** solution, three isosbestic points (0−4 equiv 367 nm, 4−12 equiv 365 nm, >12 equiv 362 nm) appeared in turn. In contrast to the former case, only one isosbestic point appeared during the titration of **DPAG1-ZnP** and **DPAG2-ZnP**. There are only four equivalent imines directly connected to the porphyrin in **DPAG1-ZnP**, so that one isosbestic point is reasonable in principle. For **DPAG2-ZnP**, two isosbestic points are expected in principle, if the coordination behavior is similar to that of **DPAG3-ZnP** and **DPAG4-ZnP**. However, only one isosbestic point was actually observed until full complexation. As a reason for this spectral change behavior, two possible explanations are considered. The first assumption is "one isosbestic point for stepwise coordination". If the intrinsic isosbestic points for each layer were almost identical, the spectral changes should have only one isosbestic point despite the stepwise complexation. An isosbestic point wavelength is defined by many transition components, for example, the $\pi-\pi^*$ absorption bands of the free base phenylazomethines, coordinating phenylazomethines, and a zinc porphyrin core. Therefore, a precise explanation of the isosbestic point is very difficult. The second assumption is "simultaneous coordination with multiple intrinsic isosbestic points". We cannot determine which assumptions are appropriate for the **DPAG2-ZnP** only by the isosbestic point determination. However, the stepwise coordination from the core side imines is indicated from the detailed analysis of the absorbance change during the titration.[27] This issue will be discussed again in the next section by employing other techniques.

(27) When the equilibrium system was defined as a two-layer system in which the coordination constants were made 5.0×10^6 [mol^{-1} L] and 2.5×10^5 [mol^{-1} L], the fitting of the titration curve was successful. In contrast, we could not fit the titration curve using the equally coordinating system, in which the metal ions coordinate to all ligands with the same constant.

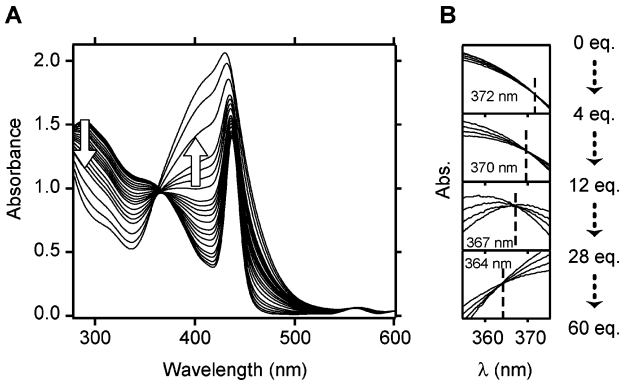

Figure 4. (A) Subtracted UV−vis absorption spectra changes of **DPAG4-ZnP** (2.5 μM) in C_6H_6/MeCN (1:1) upon the addition of $FeCl_3$, and (B) enlargements of the spectra at the isosbestic points.

The complexation of $FeCl_3$ to **DPAG4-ZnP** was also stepwise similar to that of $SnCl_2$. Four different isosbestic points were observed by subtraction of the $FeCl_3$ absorption as well as the previous experiment using **DPAGX-PPh**.[28] The absorption changes in $FeCl_3$ itself are not considered here, but they are systematically included in the absorption changes of the phenylazomethines. The subtraction does not prevent us from a qualitative analysis of the stepwise complexation behavior by the shift in the isosbestic points. The subtracted spectra upon the addition of $FeCl_3$ as shown in Figure 4 are nearly identical to the case of $SnCl_2$. Four isosbestic points were successively observed, and a similar stepwise complexation shown in Scheme 1 is also expected. The $FeCl_3$ coordination to **DPAG2-ZnP** or **DPAG3-ZnP** is not an exception.

These dendrimers can assemble not only $SnCl_2$ or $FeCl_3$, but also every metal ion or proton having a strong Lewis acidity. The coordination involves similar spectral changes in which the absorption of the coordinated phenylazomethines around 400 nm increases as well.

Electrochemical Characterization by Probing Redox Potential of the Zinc Porphyrin Core. The UV−vis absorption corresponding to the $\pi-\pi^*$ transition of the phenylazomethine units showed a drastic change by the complexation of metals ($SnCl_2$ or $FeCl_3$). The spectral changes corresponding to the porphyrin Soret band at 430 nm are also observed, but the peak shift was too small to characterize the coordination effect. It is related to the insensitiveness of the Soret band toward substitutions on the *meso*-position of the porphyrin ring. In contrast, the redox potential of the zinc porphyrin ring clearly reflects the effect by the *meso*-substitution. This property is typical of redox switching materials in host−guest chemistry.[29] For the redox-active molecules bearing some receptors, the redox potential can be reversibly switched by the complexation of inorganic or organic guest molecules. The switching property is generally based on the electronic effect by covalent bonds connecting the receptors to the redox center.

The zinc porphyrin core shows two quasi-reversible redox waves on a cyclic voltammogram. Each of them is characterized as a $1e^-$ oxidation to the monocation radical (ZnP^+) and dication (ZnP^{2+}), respectively. For **DPAG1-ZnP**, the observed half-wave potentials (middle value of the anodic and cathodic peak: $E_{1/2}$

(28) Nakajima, R.; Tsuruta, M.; Higuchi, M.; Yamamoto, K. *J. Am. Chem. Soc.* **2004**, *126*, 1630−1631.
(29) Boulas, P. L.; Gómez-Kaifer, M.; Echegoyen, L. *Angew. Chem., Int. Ed.* **1998**, *37*, 216−247.

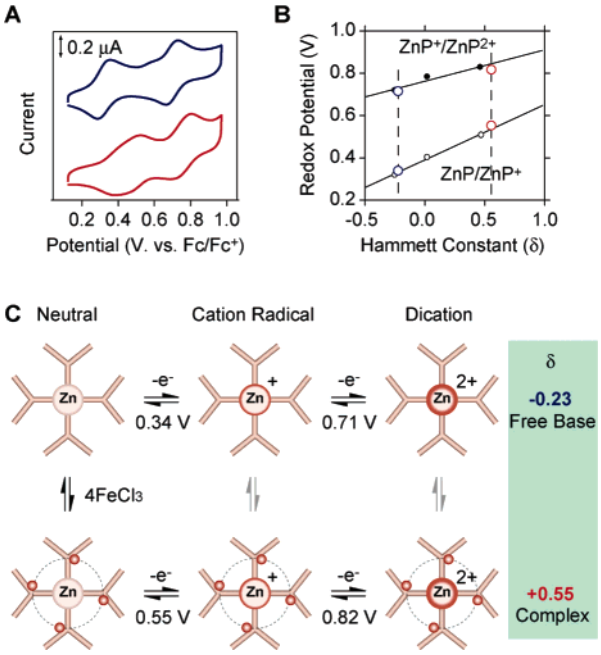

Figure 5. (A) Cyclic voltammograms of **DPAG1-ZnP** in the absence (blue) or presence (red) of 4 molar amounts of $FeCl_3$ in $CHCl_3$/MeCN (4:1) solution containing 0.1 M Bu_4NPF_6. (B) The Hammett relationship between the Hammett constant and the two redox potentials was obtained by the cyclic voltammetry measurements. The black and white plots represent the redox potentials of the zinc tetraphenyl-porphyrins (ZnTPPs) having known substituents (−OMe, −H, −COOMe). The blue and red plots correspond to the results of the free base and coordinated **DPAG1-ZnP**, respectively. The Hammett constants of **DPAG1-ZnP** are fixed to the displayed values to have each redox potential agree with the ZnTPPs. (C) A schematic representation of the redox and complexation reaction for **DPAG1-ZnP**.

$= (E_{pa} + E_{pc})/2$ of the ZnP/ZnP^+ redox couple shifted by +0.21 V after full complexation of $FeCl_3$ (Figure 5A), while the ZnP^+/ZnP^{2+} redox also shifted by +0.11 V. Each redox potential shift continued until full complexation to the four molar amounts of $FeCl_3$. The positive shift is attributed to the coordination of $FeCl_3$ to four imine units involving electron withdrawing through covalent bonds.

This effect was evaluated by comparison with the substituent effect of the *para*-substituted *meso*-tetraphenyl pophyrin zinc (**R-ZnP**) using the known Hammett constants of various molecular groups. The redox potentials of **R-ZnP** (R = OMe, H, and COOMe) were first measured to plot a calibration line for the relationship between the redox potential and the Hammett constant. Using this relationship, the Hammett constants of the free base dendron and the $FeCl_3$ complex were obtained. The analysis was applied to the redox behavior of **DPAG1-ZnP** (Figure 5B). The result indicates that the electronic effect by the phenylazomethine dendron would change from weak electron donating ($\delta = -0.23$ for free base) to strong electron withdrawing ($\delta = 0.55$ for $FeCl_3$ complex). The analysis using the Hammett constant shows that the complexation to the first layer (nearest to the core) directly affects the electronic status of the porphyrin core through the covalent bond.

A reversible redox wave of the free base **DPAG2-ZnP** at 0.33 V was also shifted to a more positive value (0.52 V) by the coordination of $FeCl_3$ (Figure 6). The potential shift converged with 4 molar amounts of $FeCl_3$ addition, although the number of imine sites is 12. In addition, the shift width almost agreed with that observed in the case of **DPAG1-ZnP** (+0.21 V). If the complexation was random, the redox potential

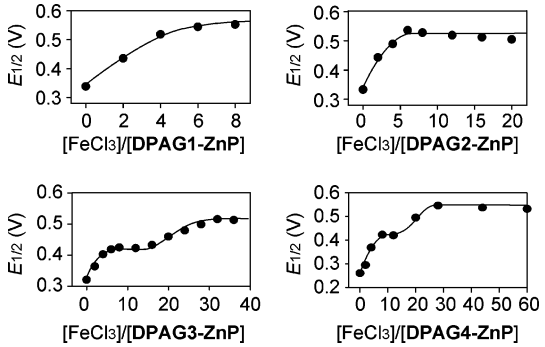

Figure 6. Variations in the half-wave potentials ($E_{1/2}$) of **DPAGX-ZnP** in $CHCl_3$/MeCN (4:1) upon the addition of $FeCl_3$.

Scheme 2. An Energy Diagram for the Oxidative Quenching of the Zinc Porphyrin S_1 State by Coordinating $FeCl_3$

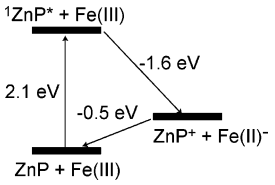

should increase until the addition of 12 molar amounts of $FeCl_3$. This result clearly shows the stepwise complexation from the inner 4 imines. This also indicates a small interaction between the core and peripheral imines.

The potential shift behavior of a larger dendrimer also converged up to the 4 equivalent ratio of $FeCl_3$. For **DPAG3-ZnP**, the ZnP/ZnP^+ redox couple shifted from 0.32 V until the addition of 4 molar amounts of $FeCl_3$. After convergence of the redox potential at 0.42 V, it shifted to 0.52 V again with the addition of 20 equivalents of $FeCl_3$. This unexpected shift is probably related to the large environmental change around the porphyrin core by the metal assembly on the surface layers of the dendrimer.[30] A similar behavior was observed in the case of **DPAG4-ZnP**. In each dendrimer, the redox shift behaviors are related to the stepwise complexation from the core-side imines, which are also characterized by the UV−vis titration method.

Probing Fluorescence Intensity of the Zinc Porphyrin Core. The fluorescence spectra of **DPAGX-ZnP** upon excitation at the Q-band of the porphyrin core are characteristic of the zinc porphyrin. The singlet-excited state (S_1) of **DPAG4-ZnP** (2.1 eV) is a weak oxidant ($E = 0.3$ V vs Fc/Fc^+) and a strong reductant ($E = -1.8$ V vs Fc/Fc^+). A redox reaction of the free base phenylazomethines with the singlet excited zinc porphyrin core ($^1ZnP^*$) does not proceed because of their lower reduction potential (> −2.0 V vs Fc/Fc^+) and higher oxidation potential (<1.0 V vs Fc/Fc^+). However, the complexation of $FeCl_3$ results in new acceptable electron levels on the phenylazomethine structure. The electron transfer from the excited zinc porphyrin to the coordinating $FeCl_3$ can be consequently promoted due to the higher reduction potential of the coordinating $FeCl_3$ (ca. −0.2 V vs Fc/Fc^+) as compared to the $^1ZnP^*$ oxidation potential (Scheme 2). The idea is consistent with the fluorescence quenching upon the addition of $FeCl_3$ to the

(30) The main reason for the environmental change should be switching of the entire conformation of the dendrimer through the complexation. It can be observed as the change in the molecular size by DLS (dynamic light scattering) measurements (in Supporting Information).

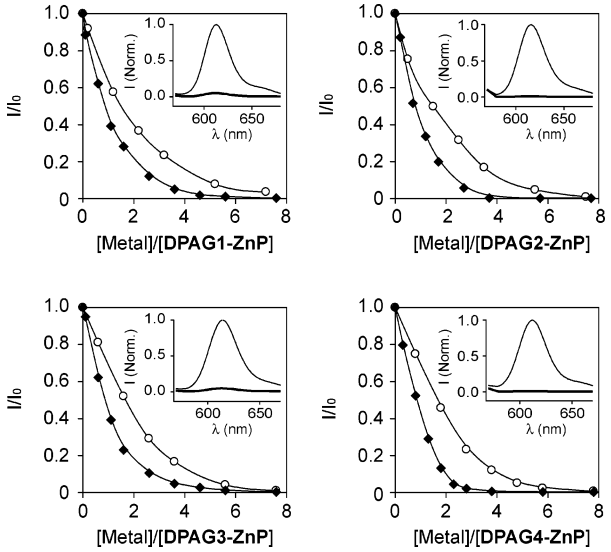

Figure 7. Normalized fluorescence intensities of **DPAGX-ZnP** (10 μM) in C_6H_6/MeCN (1:1) upon the addition of $SnCl_2$ (○) or $FeCl_3$ (◆). The emission wavelengths were observed at 613 nm (G1), 616 nm (G2), 614 nm (G3), and 612 nm (G4) with excitation at 562 nm (G1), 564 nm (G2), 562 nm (G3), and 563 nm (G4), respectively. Figures in the insets represent normalized spectra of the fluorescence in the absence (normal line) or presence (bold line) of $FeCl_3$ (4 molar amounts).

solution of **DPAGX-ZnP** (Figure 7). Only the equimolar addition of $FeCl_3$ results in an effective quenching (80−90%) of the fluorescence. The fluorescence quenching may be explained by both mechanisms of excitation energy transfer[31] and electron transfer,[32] because dendrimers can generally transact each transfer process. However, the quenching by the energy transfer is ruled out in this system because the excitation energy of ^{1}ZnP* is not sufficient to excite the phenylazomethine or $FeCl_3$.[33]

A similar experiment was carried out using the model system of the G2 dendrimer in which the core (**ZnTPP**) and dendrons (**DPAG2-Ph**) are separated from each other. However, no quenching was observed when the $FeCl_3$ was added to the solution of a mixture of **ZnTPP** and **DPAG2-Ph**. This result indicates an electron-transfer quenching mechanism via an intramolecular process. The coordinating metal ion ($FeCl_3$) on the dendritic structure quenches the fluorescence from the porphyrin core. An intermolecular electron transfer between the **ZnTPP** and **DPAG2-Ph** complex should be much slower than the intramolecular electron transfer in the dendrimer architecture.

Figure 7 shows the quenching behavior at the fluorescence maximum wavelength upon the addition of $FeCl_3$ to **DPAGX-ZnP** (X = 1−4). If the $FeCl_3$ first coordinates to surface layers in **DPAG4-ZnP**, the quenching efficiency relative to the case of **DPAG1-ZnP** should be lower because of the longer D−A (porphyrin−$FeCl_3$) distance. The quenching efficiencies are actually equal to or higher than that for the lower generation number (X). It is also evidence for the stepwise complexation from the inner imine.

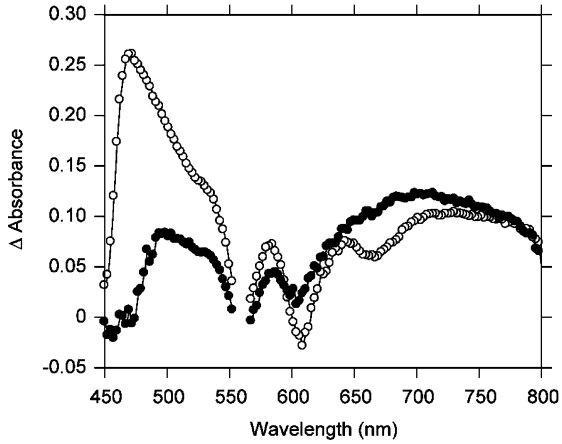

Figure 8. Transient absorption spectra of **DPAG4-ZnP** (50 μM) in the presence (●) or absence (○) of a 4 molar amount of $FeCl_3$. The spectra were obtained at 3 ps after the photoexcitation with 560 nm laser pulses in C_6H_6/MeCN (1:1) solution.

The high quenching efficiency with low molar amounts of $FeCl_3$ indicates a very fast electron transfer within the dendritic architecture. Because the fluorescence lifetime of zinc porphyrins is known to be 2−3 ns,[34,35] the electron-transfer kinetics to a coordinating $FeCl_3$ on the first layer should occur within a much shorter time scale ($\ll 10^9$ s^{-1}). In the fluorescence dendrimers reported by Vögtle and Balzani et al., the electron transfer depends on the metal ion loaded in the molecule.[9e,f] In our case, the quenching rate by the coordinating $SnCl_2$ is much lower than that with $FeCl_3$. This is due to the low reduction potential of $SnCl_2$ (Sn^0/Sn^{2+}). Based on these experiments, the phenylazomethine dendrimer was demonstrated to have a tunable electron-transfer property by varying the number and type of metal ions.

Direct Observation of the Electron Transfer by Transient Absorption Measurements. The transient absorption spectra of **DPAG4-ZnP** in the presence or absence of a four-molar amount of $FeCl_3$ were measured to support the ultrafast electron transfer in the dendrimer. As can be seen in Figure 8, the resulting chemical species of **DPAG4-ZnP** and the $FeCl_3$ complex at 3 ps after the photoexcitation (560 nm) are quite different from each other. The observed transient spectrum taken without $FeCl_3$ was very similar to that for the singlet-excited state of the zinc tetraphenyl porphyrin (^{1}ZnP*),[36] showing a characteristic large absorption peak around the wavelength of 450−550 nm and a broad absorption over 650 nm. This is evidence for the ^{1}ZnP* formation in the phenylazomethine dendrimers. The transient species of **DPAG4-ZnP** with a four-molar amount of $FeCl_3$ showed a different spectrum from ^{1}ZnP* with a smaller absorption at 500 nm and larger absorption at

(31) (a) Maus, M.; De, R.; Lor, M.; Weil, T.; Mitra, S.; Wiesler, U.-M.; Herrmann, A.; Hofkens, J.; Vosch, T.; Müllen, K.; De Schryver, F. C. *J. Am. Chem. Soc.* **2001**, *123*, 7768−7676. (b) Varnavski, O. P.; Ostrowski, J. C.; Sukhomlinova, L.; Twieg, R. J.; Bazan, G. C.; Goodson, T., III. *J. Am. Chem. Soc.* **2002**, *124*, 1736−1743. (c) Ranasinghe, M. I.; Wang, Y.; Goodson, T., III. *J. Am. Chem. Soc.* **2003**, *125*, 5258−5259. (d) Wang, Y.; Ranasinghe, M. I.; Goodson, T., III. *J. Am. Chem. Soc.* **2003**, *125*, 9562−9563.

(32) (a) Choi, M.-S.; Aida, T.; Luo, H.; Araki, Y.; Ito, O. *Angew. Chem., Int. Ed.* **2003**, *42*, 4060−4063. (b) Ghaddar, T. H.; Wishart, J. F.; Thompson, D. W.; Whitesell, J. K.; Fox, M. A. *J. Am. Chem. Soc.* **2002**, *124*, 8285−8289. (c) Lor, M.; Thielemans, J.; Viaene, L.; Cotlet, M.; Hofkens, J.; Weil, T.; Hampel, C.; Müllen, K.; Verhoeven, J. W.; Van der Auweraer, M.; De Schryver, F. C. *J. Am. Chem. Soc.* **2002**, *124*, 9918−9925.

(33) No significant absorption band appears in the region of a wavelength longer than the fluorescence band of the zinc porphyrin core (616 nm).

(34) (a) Kalyanasundaram, K. *Photochemistry of Polypyridine and Porphyrin Complexes*; Academic Press: London, 1992. (b) Da Ros, T.; Prato, M.; Guldi, D. M.; Alessio, E.; Ruzzi, M.; Pasimeni, L. *Chem. Commun.* **1999**, 635−636. (c) Luo, C.; Imahori, H.; Tamaki, K.; Sakata, Y. *J. Am. Chem. Soc.* **2000**, *122*, 6535−6551.

(35) The fluorescence lifetimes of **DPAGX-ZnP** (X = 1−4) were determined to be 1.8 ns (G1), 2.1 ns (G2), 2.2 ns (G3), and 2.3 ns (G4).

(36) Rodriguez, J.; Kirmaier, C.; Holten, D. *J. Am. Chem. Soc.* **1989**, *111*, 6500−6506.

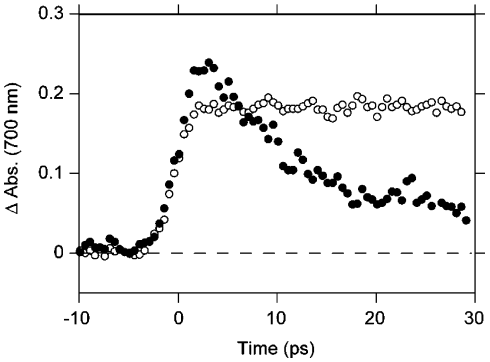

Figure 9. Transient absorption time-courses of **DPAG4-ZnP** (50 μM) in the presence (●) or absence (○) of a 4 molar amount of $FeCl_3$. They were obtained at 700 nm after the photoexcitation with 560 nm laser pulses in a C_6H_6/MeCN (1:1) solution.

700 nm. The broad absorption peak at 700 nm is characteristic of the zinc porphyrin cation radical observed during the electrochemical oxidation of **DPAG4-ZnP**. It is noteworthy that the charge separating state had already formed within a few picoseconds. This result suggests the femto-second kinetics of the electron transfer from the excited zinc porphyrin core. Goodson et al. reported that organic dendrimers are capable of controlling the photoinduced ultrafast excited energy transfer dynamics based on their unique architecture.[37] The kinetics are close to the nuclear vibration time scale, so that adiabatic electron transfer through a covalent bond should control the entire ET process. The quantum yield of the porphyrin cation radical from the ^{1}ZnP* is about 80−90%, which was estimated from the breaching intensity of the ground-state absorption at 605 nm.

The oxidized state of the porphyrin core quickly decayed within a few picoseconds. The absorption decay curves obtained at 700 nm are shown in Figure 9. In the absence of $FeCl_3$, the transient absorption did not decay within 30 ps, because the lifetime of the ^{1}ZnP* is usually longer than nanoseconds. In the presence of $FeCl_3$, **DPAG4-ZnP** showed the first-order decay of the absorption (700 nm) with the lifetime of $\tau = 8.6$ ps. At 100 ps after the excitation, no transient species could be observed at all. This means that the charge separating state between the core and assembling metal ions results in charge recombination within 100 ps. The kinetics of the electron transfer are appropriate by consideration of the D−A distance if the four metal ions are coordinating to the layer nearest to the core.[38] It is noteworthy that the further addition of $FeCl_3$ to the dendrimer does not change the fast decay kinetics of the charge separation. If the complexations were random, the decay lifetime should change. This is direct evidence for the stepwise complexation from the inner imines.

Conclusion

We synthesized and characterized a series of phyenylazomethine dendrimers with a metallo-porphyrin core. The fourth generation dendrimer has an ca. 5 nm diameter sphere-like structure, which is supported by both the experimental value ($R_h = 2.2$ nm, by TriSEC) and the molecular modeling calculations. Although the dendrimer showed an encapsulating effect on the porphyrin core, it has a space in itself due to the rigid structure. Metal ion coordination to the imine units on the branches of the fouth-generation dendrimer (**DPAG4-ZnP**) was demonstrated. The stepwise radial complexation from the root imines (nearest the core) was exhibited by the UV−vis titration using $SnCl_2$ and $FeCl_3$ as the coordinating metal ions. The metal ion coordination resulted in effective switching of the redox potential of the ZnP core. The behavior was quantitatively analyzed and consistent with the stepwise radial complexation predicted by the UV−vis measurements for every generation number (X = 1−4) of the dendrimer (**DPAGX-ZnP**). Fluorescence quenching of the zinc porphyrin core in the metal ion assembled dendrimer is also noteworthy, because the phenomena are evidence for the electron transfer between the core and assembled metal ions. A comparison of the results with that of model compounds showed that the quenching is related to the intra-dendrimer electron transfer. The transient absorption measurements revealed that the phototriggered ET kinetic is faster than the picosecond time scale. The generation number dependence of the fluorescent quenching suggests again the stepwise complexation from the inner shell.

We could verify the unique complexation process shown in Scheme 1 by three different methods (UV−vis absorption, redox reaction, fluorescence). The fine control of the metal assembly around the functional porphyrin center would be important because it is applicable to many combinations of metalloporphyrins and assembled metal elements. A series of metal−organic hybrid materials called a "macromolecule−metal complex" has been applied to many categories of functional materials, such as catalysts or photoenergy conversion systems involving electron-transfer reactions. The precisely assembled metal complexes around the porphyrin could be regarded as the development of these macromolecular−metal complexes. Our current interest is focused on the application of these molecules as molecular catalysts and electronics utilizing the monodispersity in the molecular structure and complexation.

Experimental Section

General. The NMR spectra were recorded on a FT-NMR spectrometer (JEOL, JNM-GX 400) operating at 400 MHz (^{1}H) or 100 MHz (^{13}C). The ^{1}H NMR chemical shifts were referenced to the solvent peak ($CDCl_3$: 7.26 ppm) and tetramethoxysilane (TMS: 0 ppm) as internal standards. The ^{13}C NMR chemical shifts were referenced to the solvent peak ($CDCl_3$: 77.0 ppm). The ^{1}H NMR pulse relaxation times (T_1) were measured in a saturation recovery data processing mode. The MALDI-TOF-mass spectra were obtained using a mass spectrometer (Shimadzu/Kratos, AXIMA CFR plus: Positive mode). Dithranol (1,8-dihydroxy-9[10*H*]-anthracenone) was used as the matrix for the MALDI-TOF-mass measurements. A preparative recycling HPLC (Japan Analytical Industry: LC908) was used for the purification of the dendrimers with chloroform or THF as the eluent at the flow rate of 3.5 mL/min.

A field-emission transmission electron microscope (FE-TEM) image was obtained using a TECNAI F20 (FEI). RuO_4 was used as the staining agent to enhance the electron density contrast of the FE-TEM.[39] Analytical size-exclusion chromatography (SEC) was performed using an HPLC (Shimadzu, LC-10AP) equipped with a TSK-GEL CMHXL (Tosoh) at 40 °C. Tetrahydrofran (THF) was used as the eluent at the flow rate of 1 mL/min. The detection line was connected to a triple detector (Viscotek, TriSEC model 302). The semi-empirical molecular orbital calculations and optimizations of the molecular conformation

(37) (a) Goodson, T., III. *Acc. Chem. Res.* **2005**, *38*, 99−107. (b) Goodson, T., III. *Annu. Rev. Phys. Chem.* **2005**, *56*, 581−603.
(38) Yu, H.-Z.; Baskin, S.; Steiger, B.; Anson, F. C.; Zewail, A. H. *J. Am. Chem. Soc.* **1999**, *121*, 484−485.
(39) Trent, J. S.; Scheinbeim, J. I.; Couchman, P. R. *Macromolecules* **1983**, *16*, 589−598.

were done on a Cache Worksystem ver. 5.04 (Fujitsu) employing the MOPAC-AM1 parameter.

The UV−vis absorption spectra were recorded using a UV-3100PC (Shimadzu) with a sealed quartz cell (d = 1 cm). The fluorescence spectra were measured using a FP-6500 spectrophotometer (JASCO). Cyclic voltammograms were recorded using an 660A electrochemical analyzer (ALS). A glassy carbon electrode (ϕ = 3 mm) was used as the working electrode, which was polished with 0.05 mm alumina paste before the analysis. A coiled platinum wire was used as the counter electrode. A silver wire electrode dipped in 0.01 M $AgNO_3$ + 0.1 M Bu_4NClO_4/CH_3CN solution was used as the potential reference (Ag/Ag^+). The redox potential was then referenced to the ferrocene/ferrocenium (Fc/Fc^+) standard by the half-wave potential of 0.2 mM ferrocene measured in 0.1 M Bu_4NClO_4/CH_3CN.[40] The UV−vis absorption spectra of the electrochemically oxidized species were measured using the same setup with a custom-made quartz cell (d = 1 mm). A platinum mesh inserted into the optical path was used as the working electrode.

Transient Absorption Measurements. The laser system used for the picosecond transient absorption spectra and decays is the same as that used in previous experiments.[41] It is based on a cw mode-locked Ti:sapphire laser (Spectra Physics, Tsunami) with a pulse duration of 130 fs pumped by a 5 W diode laser (Spectra Physics, Millennia Vs). The output pulses (550 mW; 82 MHz) from the oscillator are amplified at the repetition rate of 10 Hz in a regenerative Ti:sapphire amplifier (Quanta Ray, TSA-10) pumped by the frequency-doubled output of a Nd^{3+}:YAG laser (Quanta Ray, Pro-230). By masking the grating in a regenerative Ti:sapphire amplifier, the time duration and energy of the amplified output pulses were ∼3 ps and 5.5 mJ/pulse at 800 nm, respectively. The output was divided into two beams. One beam was used to pump a traveling-wave optical parametric amplifier (OPA) system (light conversion, TOPAS 400) after frequency doubling in BBO and to provide 560 nm pulses by the signal wave from the OPA. The 560 nm pulses were focused on the sample solution in a quartz cell (d = 1 cm). The other beam was used to probe the absorptions of the excited sample. The delay time between the pump and probe laser was varied by an optical delay system (Sigma, LTS-400X; 5 μm/step).

For the multichannel measurements of the absorption spectra, the probe pulses (800 nm) were focused into a D_2O cell to generate white light by the self-phase modulation (SPM) effect. The white pulses were passed through a notch filter (800 nm) and split into two beams for the sample and reference (for intensity compensation of the laser system). The two beams that passed from these samples were directed to a single polychromator (Jobin Yvon, HR-320) by optical fibers with a notch filter (560 nm) as a pump dumper and detected by ICCD (Princeton Instruments Inc.: PI-MAX-512).

For the single-channel measurements of the decay profiles, the probe pulses (800 nm) were converted to 500 and 700 nm. The 500 nm pulses were obtained as the fourth harmonics of the idler wave from the OPA (light conversion, TOPAS 800). The 700 nm pulses were obtained as the second harmonics of the signal wave from the OPA (TOPAS 800). The detection line was similar to that for the multichannel measurements. The divided two beams were detected by two separate photomultipliers (Hamamatsu, 1P28).

Materials. Tin(IV) chloride, 1,4-diazabicyclo[2.2.2]octane (DABCO), benzophenone, chlorobenzene, and all solvents used for the purifications were purchased from Kantoh Kagaku Co. Tetrahydrofuran (THF) for the HPLC analysis and cyclic voltammetry was HPLC grade from Kantoh Kagaku Co. without any stabilizer. All other solvents for the measurements were of dehydrated grade for organic synthesis from Kantoh Kagaku Co. Dehydrated $SnCl_2$ and $FeCl_3$ were purchased from Wako Pure Chemicals Co. and Merck, respectively. 5,10,15,20-Tetrakis-(4-aminophenyl)porphine (**NH_2-H_2P**) was synthesized by a literature method.[10] All of the DPA dendrons (G2−G4) and a model compound (**DPAG2-Ph**) were synthesized as previously described. All of the **DPAGX-ZnP**s (X = 1−4) were synthesized via **DPAGX-H_2P** followed by insertion of zinc into the porphyrin ring. The detailed procedures are described below.

Synthesis of DPAG1-ZnP. NH_2-H_2P (60 mg, 0.088 mmol), benzophenone (98 mg, 0.54 mmol), and DABCO (240 mg, 2.12 mmol) were dissolved in chlorobenzene (20 mL). Titanium(IV) chloride (57 μL, 0.52 mmol) in chlorobenzene (2 mL) was slowly added through a dropping funnel under N_2. The reaction mixture was heated at 125 °C for 3 h. The precipitate was removed by filtration, and the solution was concentrated to dryness. **DPAG1-H_2P** (50 mg, 0.037 mmol, 42%) was isolated by silica gel (neutral) column chromatography (hexane:chloroform:ethyl acetate = 10:10:1). The product was purified by a preparative recycling HPLC (LC-908 with JAIGEL-1H + JAIGEL-2H) with chloroform as the eluent. **DPAG1-H_2P**: ^{1}H NMR ($CDCl_3$) δ 8.71 (s, 8H), 7.96 (d, 8H, J = 7.8 Hz), 7.94 (d, 8H, J = 7.8 Hz), 7.58−7.51 (m, 24H), 7.43(dd, 8H), 7.10 (d, 8H, J = 7.6 Hz), −2.88 (s, 2H); ^{13}C NMR ($CDCl_3$) δ 169.09, 151.04, 139.32, 136.84, 136.31, 134.41, 130.85, 129.73, 129.36, 128.78, 128.21, 127.89, 119.64, 119.06; MALDI-TOF-mass calcd 1331.54 $[M + H]^+$, found 1331.09; UV−vis (λ_{max} nm, $CHCl_3$, 5 μmol L^{-1}) 426, 520, 556, 595, 650. Anal. Calcd for $C_{96}H_{66}N_8$: C, 86.59; H, 5.00; N, 8.41. Found: C, 86.31; H, 5.02; N, 8.30. **DPAG1-H_2P** (50 mg, 0.037 mmol), zinc acetate (22 mg, 0.12 mmol), and triethylamine (0.5 mL) were dissolved in dehydrated THF (25 mL). The reaction mixture was refluxed under a N_2 atmosphere for 3 h. The reaction was monitored by the disappearance of the free-base porphyrin Q-band (650 nm) by the UV−vis spectrum. The resulting mixture was concentrated and dropped into methanol. The precipitate was then collected by filtration and dried after washing with methanol and hexane. The product was further purified by a preparative recycling HPLC (LC-908 with JAIGEL-1H + JAIGEL-2H) with THF as the eluent, which produced 47 mg of **DPAG1-ZnP** (76%). **DPAG1-ZnP**: ^{1}H NMR ($CDCl_3$) δ 8.82 (s, 8H), 7.97 (d, 8H, J = 8.0 Hz), 7.95 (d, 8H, J = 8.0 Hz), 7.57−7.51 (m, 24H), 7.43 (dd, 8H), 7.10 (d, 8H, J = 8.4 Hz); ^{13}C NMR (100 MHz, $CDCl_3$, TMS) δ 169.05, 150.88, 150.03, 139.38, 137.50, 136.37, 134.25, 131.53, 129.76, 129.36, 128.78, 128.21, 127.89, 125.36, 120.65, 118.95; MALDI-TOF-mass calcd 1395.98 $[M + H]^+$, found 1395.46; UV−vis (λ_{max} nm, $CHCl_3$, 5 μmol L^{-1}) 429, 554, 596.

Synthesis of DPAG2-ZnP. NH_2-H_2P (200 mg, 0.29 mmol), the DPA dendron G2 800 mg (1.48 mmol), and DABCO (799 mg, 7.12 mmol) were dissolved in chlorobenzene (50 mL). Titanium(IV) chloride (195 μL, 1.78 mmol) in chlorobenzene (10 mL) was slowly added through a dropping funnel under N_2. The reaction mixture was heated at 125 °C for 3 h. The precipitate was removed by filtration, and the solution was concentrated to dryness. **DPAG2-H_2P** (396 mg, 0.14 mmol, 48%) was isolated by silica gel (neutral) column chromatography (dichloromethane:ethyl acetate = 40:3 including triethylamine 0.5%). The product was purified by preparative recycling HPLC (LC-908 with JAIGEL-1H + JAIGEL-2H) with chloroform as the eluent. **DPAG2-H_2P**: ^{1}H NMR ($CDCl_3$) δ 8.81 (s, 8H), 7.92 (d, 8H, J = 8.4 Hz), 7.80 (d, 8H, J = 6.8 Hz), 7.69 (d, 8H, J = 8.4 Hz), 7.66 (d, 8H, J = 8.4 Hz), 7.52 (t, 4H, J = 7.4 Hz), 7.45 (d, 8H, J = 7.4 Hz), 7.36 (m, 24H), 7.2 (dd, 8H, J = 6.8, 8.4 Hz), 7.08 (d, 8H, J = 8.4 Hz), 7.03 (d, 8H, J = 7.2 Hz), 6.96 (d, 8H, J = 8.0 Hz), 6.84 (d, 8H, J = 8.4 Hz), 6.80 (d, 8H, J = 7.6 Hz), 6.76 (d, 8H, J = 8.4 Hz), 6.55 (d, 8H, J = 7.4 Hz), −2.70(s, 2H); ^{13}C NMR ($CDCl_3$) δ 168.84, 168.41, 168.36, 153.61, 152.01, 151.12, 138.95, 136.55, 135.57, 134.62, 132.29, 130.87, 130.82, 130.51, 130.14, 129.94, 129.42, 129.35, 129.25, 129.15, 128.38, 128.15, 128.01, 127.55, 120,54, 120.16, 120.02, 119.63; MALDI-TOF-mass calcd 2764.13 $[M + H]^+$, found 2762.61; UV−vis (λ_{max} nm, $CHCl_3$, 5 μmol L^{-1}) 287, 430, 521, 560, 594, 652. Anal. Calcd for $C_{200}H_{138}N_{16}$: C, 86.87; H, 5.03; N, 8.10. Found: C, 86.76; H, 5.03; N, 8.01. **DPAG2-H_2P** (101 mg, 0.036 mmol), zinc acetate (29 mg, 0.16

(40) Pavilishchuk, V. V.; Addison, A. W. *Inorg. Chim. Acta* **2000**, *298*, 97−102.
(41) (a) Sakai, M.; Ishiuchi, S.; Fujii, M. *Eur. Phys. J. D* **2002**, *20*, 399−402. (b) Sakai, M.; Fujii, M. *Chem. Phys. Lett.* **2004**, *396*, 298−302.

mmol), and triethylamine (0.5 mL) were dissolved in dehydrated THF (30 mL). The reaction mixture was refluxed under a N_2 atmosphere for 3 h. The reaction was monitored by the disappearance of the free-base porphyrin Q-band (650 nm) in the UV−vis spectrum. The resulting mixture was concentrated and dropped into a methanol. The precipitate was then collected by filtration and dried after washing with methanol and hexane. The product was purified by preparative recycling HPLC (LC-908 with JAIGEL-1H + JAIGEL-2H) with THF as the eluent, which produced 69 mg of **DPAG2-ZnP** (67%). **DPAG2-ZnP**: ^{1}H NMR ($CDCl_3$) δ 8.91 (s, 8H), 7.93 (d, 8H, J = 8.4 Hz), 7.80 (d, 8H, J = 7.6 Hz), 7.70 (d, 8H, J = 8.4 Hz), 7.66 (d, 8H, J = 8.0 Hz), 7.51 (t, 4H, J = 7.4 Hz), 7.45 (t, 8H, J = 7.4 Hz), 7.36 (m, 24H), 7.3 (dd, 8H, J = 7.6, 6.8 Hz), 7.08 (d, 8H, J = 8.4 Hz), 7.04 (d, 8H, J = 7.4 Hz), 6.96 (d, 8H, J = 8.2 Hz), 6.83 (d, 8H, J = 7.4 Hz), 6.81 (d, 8H, J = 7.6 Hz), 6.76 (d, 8H, J = 7.6 Hz), 6.56 (t, 8H, J = 7.6 Hz); ^{13}C NMR ($CDCl_3$) δ 168.78, 168.36, 168.26, 153.54, 152.01, 151.95, 150.88, 150.13, 139.24, 138.94, 137.16, 135.80, 135.54, 134.65, 134.43, 131.76, 130.81, 130.50, 130.08, 129.89, 129.37, 129.31, 129.21, 129.13, 128.76, 128.29, 128.11, 128.07, 127.97, 127.50, 120,95, 120.48, 120.11, 119.45; MALDI-TOF-mass calcd 2829.73 $[M + H]^+$, found 2829.93; UV−vis (λ_{max} nm, $CHCl_3$, 5 μmol L^{-1}) 285, 433, 556, 599.

Synthesis of DPAG3-ZnP. NH_2-H_2P (146 mg, 0.22 mmol), the DPA dendron G3 (1.65 g, 1.30 mmol), and DABCO (1.00 g, 8.91 mmol) were dissolved in chlorobenzene (100 mL). Titanium(IV) chloride (142 μL, 1.30 mmol) in chlorobenzene (3 mL) was slowly added through a dropping funnel under N_2. The reaction mixture was heated at 125 °C for 3 h. The precipitate was removed by filtration, and the solution was concentrated to dryness. The product was chromatographed on silica gel (neutral, hexane:dichloromethane:ethyl acetate = 3:3:1 including triethylamine 0.5%) to remove any remaining titanyl complex and half-finished products. The crude product (**DPAG3-H_2P**), zinc acetate (100 mg, 0.54 mmol), and triethylamine (0.5 mL) were dissolved in dehydrated THF (50 mL). The reaction mixture was refluxed under a N_2 atmosphere for 3 h. The reaction was monitored by the disappearance of the free-base porphyrin Q-band (650 nm) in the UV−vis spectrum. The resulting mixture was concentrated and dropped into methanol. The precipitate was then collected by filtration and dried after washes with methanol and hexane. The product was further purified by preparative recycling HPLC (LC-908 with JAIGEL-2H + JAIGEL-3H) with THF as the eluent, which produced 517 mg of **DPAG3-ZnP** (42% from **NH_2-ZnP**). **DPAG3-ZnP**: ^{1}H NMR ($CDCl_3$) δ 8.89 (s, 8H), 7.95 (d, 8H, J = 8.0 Hz), 7.78 (d, 8H, J = 8.0 Hz), 7.73 (d, 8H, J = 7.6 Hz), 7.69 (d, 8H, J = 7.4 Hz), 7.55−7.15 (m, 112H), 7.09−7.02 (m, 24H), 6.97 (d, 8H, J = 7.6 Hz), 6.92−6.89 (m, 20H), 6.80 (d, 8H, J = 8.2 Hz), 6.77 (d, 8H, J = 8.2 Hz), 6.72 (d, 24H, J = 8.2 Hz), 6.67 (d, 8H, J = 8.2 Hz), 6.59 (d, 8H, J = 8.0 Hz), 6.58 (t, 4H), 6.46 (d, 8H, J = 7.6 Hz), 6.29 (d, 8H, J = 8.2 Hz); ^{13}C NMR ($CDCl_3$) δ 168.85, 168.49, 168.36, 168.17, 167.98, 167.93, 167.78, 153.92, 153.59, 152.42, 151.82, 151.44, 150.68, 149.84, 139.20, 139.12, 139.00, 137.82, 137.41, 135.74, 135.62, 135.50, 135.23, 134.52, 134.34, 134.23, 134.01, 131.60, 130.75, 130.56, 130.47, 130.33, 130.26, 130.10, 130.01, 129.95, 129.31, 129.25, 128.81, 128.27, 128.10, 128.07, 127.93, 127.85, 127.45, 127.16, 120.79, 120.62, 120.42, 120.21, 119.91, 119.59; MALDI-TOF-mass calcd 5696.81 $[M + H]^+$, found 5697.20; UV−vis (λ_{max} nm, $CHCl_3$, 5 μmol L^{-1}) 288, 435, 556, 599.

Synthesis of DPAG4-ZnP. NH_2-H_2P (35 mg, 0.051 mmol), the DPA dendron G4 (704 mg, 0.26 mmol), and DABCO (674 mg, 6.00 mmol) were dissolved in chlorobenzene (50 mL). Titanium(IV) chloride (50 μL, 0.46 mmol) in chlorobenzene (1 mL) was added through a dropping funnel under N_2. The reaction mixture was heated at 125 °C for 3 h. The precipitate was removed by filtration, and the solution was concentrated to dryness. The product was chromatographed on silica gel (neutral, hexane:dichloromethane:ethyl acetate = 2:2:1 including triethylamine 0.5%) to remove any remaining half-finished products. The crude product (**DPAG4-H_2P**), zinc acetate (59 mg, 0.32 mmol), and triethylamine (0.5 mL) were dissolved in dehydrated THF (30 mL). The reaction mixture was refluxed under a N_2 atmosphere for 3 h. The reaction was monitored by the disappearance of the free-base porphyrin Q-band (650 nm) in the UV−vis spectrum. The resulting mixture was concentrated and dropped into methanol. The precipitate was then collected by filtration and dried after washing with methanol and hexane. The product was purified by preparative recycling HPLC (LC-908 with JAIGEL-2H + JAIGEL-3H) with THF as the eluent, which produced 280 mg of **DPAG4-ZnP** (46% from **NH_2-ZnP**). **DPAG4-ZnP**: ^{1}H NMR ($CDCl_3$) δ 8.77 (br, 8H), 7.8−6.4 (m, 536H), 6.19 (br, 16H), 5.85 (br, 8H); ^{13}C NMR ($CDCl_3$) δ 168.91, 168.75, 168.40, 168.21, 168.11, 167.81, 154.02, 153.65, 153.57, 152.24, 151.88, 151.78, 149.99, 139.22, 139.12, 138.87, 137.47, 135.70, 135.53, 134.72, 134.39, 134.24, 134.19, 134.11, 133.78, 133.62, 132.31, 130.86, 130.75, 130.47, 130.34, 130.06, 129.96, 129.80, 129.64, 129.34, 128.79, 128.61, 128.17, 128.09, 127.96, 127.84, 127.78, 127.55, 126.36, 121.09, 120.85, 120.62, 120.46, 120.23, 120.04, 119.63; MALDI-TOF-mass calcd 11 432.16 $[M + H]^+$, found 11 431.40; UV−vis (λ_{max} nm, $CHCl_3$, 5 μmol L^{-1}) 285, 437, 559, 602.

Acknowledgment. This work was supported in part by the Core Research for Evolutional Science and Technology (CREST) program of the Japan Science and Technology (JST) Agency, by a Scientific Research Program for the 21st Century Center of Excellence (COE) (Keio-LCC) of the Ministry of Education, Culture, Sports, Science, and Technology (MEXT) of Japan, and by a research grant (Project No. 23) from Kanagawa Academy of Science and Technology (KAST).

Supporting Information Available: Structural information, electrochemical properties, and additional data of metal ion assembly. This material is available free of charge via the Internet at http://pubs.acs.org.

JA0524797